

Article

Modulational Instability of Ion-Acoustic Waves and Associated Envelope Solitons in a Multi-Component Plasma

Subrata Banik ^{1,2,*}, Nadiya Mehzabeen Heera ¹, Tasfia Yeashna ¹, Md. Rakib Hassan ¹,
Rubaiya Khondoker Shikha ¹, Nure Alam Chowdhury ³, Abdul Mannan ¹ and A A Mamun ¹

¹ Department of Physics, Jahangirnagar University, Savar, Dhaka 1342, Bangladesh; heera112phys@gmail.com (N.M.H.); yeashna147phy@gmail.com (T.Y.); hassan148phy@gmail.com (M.R.H.); shikha261phy@gmail.com (R.K.S.); abdulmannan@juniv.edu (A.M.); mamun_phys@juniv.edu (A.A.M.)
² Health Physics Division, Atomic Energy Centre, Dhaka 1000, Bangladesh
³ Plasma Physics Division, Atomic Energy Centre, Dhaka 1000, Bangladesh; nurealam1743phy@gmail.com
* Correspondence: bsubrata.37@gmail.com

Abstract: A generalized plasma model with inertial warm ions, inertialess iso-thermal electrons, super-thermal electrons and positrons is considered to theoretically investigate the modulational instability (MI) of ion-acoustic waves (IAWs). A standard nonlinear Schrödinger equation is derived by applying the reductive perturbation method. It is observed that the stable domain of the IAWs decreases with ion temperature but increases with electron temperature. It is also found that the stable domain increases by increasing (decreasing) the electron (ion) number density. The present results will be useful in understanding the conditions for MI of IAWs which are relevant to both space and laboratory plasmas.

Keywords: ion-acoustic waves; NLSE; modulational instability; envelope solitons; super-thermality



Citation: Banik, S.; Heera, N.M.; Yeashna, T.; Hassan, M.R.; Shikha, R.K.; Chowdhury, N.A.; Mannan, A.; Mamun, A.A. Modulational Instability of Ion-Acoustic Waves and Associated Envelope Solitons in a Multi-Component Plasma. *Gases* **2021**, *1*, 148–155. <https://doi.org/10.3390/gases1030012>

Academic Editor: Ben J. Anthony

Received: 28 July 2021

Accepted: 24 August 2021

Published: 27 August 2021

Publisher's Note: MDPI stays neutral with regard to jurisdictional claims in published maps and institutional affiliations.



Copyright: © 2021 by the authors. Licensee MDPI, Basel, Switzerland. This article is an open access article distributed under the terms and conditions of the Creative Commons Attribution (CC BY) license (<https://creativecommons.org/licenses/by/4.0/>).

1. Introduction

The co-existence of electrons and positrons in an electron–positron–ion (EPI) plasma medium (EPIPM) was identified by the THEMIS mission [1] and Viking satellite [2] in both space (viz., Saturn's magnetosphere [3–7], early universe [4–6], pulsar magnetosphere [4–6], solar atmosphere [8–11], active galactic nuclei [12,13], and polar regions of neutron stars [14], etc.) and laboratory environments (viz., high intensity laser irradiation [4], semiconductor plasmas [12], hot cathode discharge [4], and magnetic confinement systems [12], etc.). A large number of authors studied ion-acoustic (IA) waves (IAWs) [3–6,8–10,15], positron-acoustic waves (PAWs) [7], and electron-acoustic waves (EAWs) [11] as well as their associated nonlinear structures such as solitons [3,4], shocks, rogue waves [9], double layers, and dark and bright envelope solitons [5] to understand the basic properties of EPIPM. Ali et al. [7] examined the PAWs in EPI magnetoplasma. Paul et al. [16] investigated the stability of the IAWs in the presence of positron.

Two-temperature electrons (hot and cold) were identified by the Voyager PLS [17] and Cassini CAPS [18] observations in Saturn's magnetosphere, and were successively verified by several satellite missions, viz., Viking Satellite [2], FAST Auroral Snapshot (FAST) at the auroral region [19] and THEMIS mission [1], and are governed by the super-thermal kappa/ κ -distribution rather than well-known Maxwellian distribution, and were also considered by many authors for analyzing the propagation of nonlinear electrostatic waves [20] in space plasmas. The super-thermal parameter (κ) in κ -distribution represents the super-thermality of plasma species, and the small values of κ determine the large deviation of the plasma species from the thermal equilibrium state of the plasma system, while for the large values of κ , the plasma system coincides with the Maxwellian distribution. Shahmansouri and Alinejad [3] considered a three-component plasma model with two-temperature super-thermal electrons and cold ions, and investigated IA solitary waves,

and confirmed the existence of both compressive and rarefactive solitary structures in the presence of the two-temperature super-thermal electrons. Baluku and Helberg theoretically and numerically analyzed IA solitons in the presence of two-temperature super-thermal electrons. Panwar et al. [8] demonstrated IA cnoidal waves in a three-component plasma medium with inertial cold ion and inertialess two-temperature κ -distributed electrons, and found that a cold electron's super-thermality increases the height of the cnoidal wave.

The MI of wave packets has been considered the basic platform for the formation of bright and dark envelope solitons in plasmas, and has also caused a number of authors to investigate the MI of electrostatic waves and associated bright and dark envelope solitons in the interdisciplinary field of nonlinear-sciences, viz., fiber telecommunications [5], oceanic wave [9], optics [9], and plasmas [6], etc. The intricate mechanism of the MI of various waves (viz., IAWs, EAWs, and PAWs, etc.) and the formation of the electrostatic envelope solitonic solitons was governed by the standard nonlinear Schrödinger equation (NLSE) [13,21]. Kourakis and Shukla [5] investigated the MI of the IAWs in a super-thermal plasma with inertial cold ion and inertialess cold and hot electrons. Alinejad et al. [6] studied the stability conditions of the IAWs in the presence of super-thermal electrons and found that the stable region of the IAWs decreases with the number density of the cold electrons. Ahmed et al. [21] examined the stability of IAWs and observed that the critical wave number k_c decreases with the increase in the value of κ .

The manuscript is organized in the following order: the governing equations of the plasma model are presented in Section 2. The derivation of NLSE by using the reductive perturbation method (RPM) is represented in Section 3. The MI and associated envelope solitons of IAWs are given in Section 4. The numerical analysis is given in Section 5. Finally, the conclusion is presented in Section 6.

2. Governing Equations

We consider a four-component unmagnetized plasma model consisting of warm ions (with charge $q_+ = Z_+e$; mass m_+), κ -distributed super-thermal electrons (with charge $q_{e1} = -e$; mass m_{e1}), iso-thermal electrons (with charge $q_{e2} = -e$; mass m_{e2}), and super-thermal κ -distributed positrons (with charge $q_p = e$; mass m_p). The overall charge neutrality at equilibrium can be expressed as $\mu_1 + \mu_2 - \mu_3 = 1$, where $\mu_1 = n_{e10}/(Z_+n_{+0})$, $\mu_2 = n_{e20}/(Z_+n_{+0})$, and $\mu_3 = n_{p0}/(Z_+n_{+0})$. Now, the basic set of normalized equations can be written in the following form:

$$\frac{\partial n_+}{\partial t} + \frac{\partial}{\partial x}(n_+u_+) = 0, \quad (1)$$

$$\frac{\partial u_+}{\partial t} + u_+ \frac{\partial u_+}{\partial x} + \eta n_+ \frac{\partial n_+}{\partial x} = -\frac{\partial \phi}{\partial x}, \quad (2)$$

$$\frac{\partial^2 \phi}{\partial x^2} + n_+ = \mu_1 n_{e1} + \mu_2 n_{e2} - (\mu_1 + \mu_2 - 1)n_p, \quad (3)$$

where n_s is the number density of plasma species s and u_+ is the ion fluid speed. The normalization is carried out by using the following variable: $n_+ \rightarrow N_+/n_{+0}$, $x \rightarrow X/\lambda_D$, $u_+ \rightarrow U_+/C_+$, $t \rightarrow T\omega_{p+}$, $\omega_{p+} = (4\pi e^2 Z_+^2 n_{+0}/m_+)^{1/2}$, and $\lambda_{D+} = (k_B T_{e1}/4\pi e^2 Z_+ n_{+0})^{1/2}$, where n_+ is the number density of inertial warm ions normalized by its equilibrium value, n_{+0} ; u_+ is the ion fluid speed normalized by the IAW speed $C_+ = (Z_+ k_B T_{e1}/m_+)^{1/2}$ (with T_{e1} being the κ -distributed electron temperature, m_+ being the ion rest mass, and k_B being the Boltzmann constant), and ϕ is the electrostatic wave potential normalized by $k_B T_{e1}/e$. The parameter η is defined as $\eta = 3T_+/(Z_+ T_{e1})$. The ion pressure is $P_+ = k_B N_+ T_+ (N_+/n_{+0})^{2/N}$, where T_+ and N is the temperature of warm ion and degrees of freedom ($N = 1$ for one dimension), respectively.

In the case of super-thermal electron and positron, the super-thermal parameter $\kappa > 3/2$ and the number density equations are as follows [6,22,23]:

$$n_{e1} = [1 - 2\phi/(2\kappa - 3)]^{(-\kappa+1/2)}, \quad (4)$$

$$n_p = \left[1 + 2\rho\phi / (2\kappa - 3) \right]^{(-\kappa+1/2)}, \quad (5)$$

where $\rho = T_{e1}/T_p$ (with T_p being the super-thermal positron temperature). We express the number density equation of iso-thermal distributed electron as follows:

$$n_{e2} = \exp(\varrho\phi), \quad (6)$$

where $\varrho = T_{e1}/T_{e2}$ is greater than 1 and T_{e2} is the iso-thermal electron temperature. Now, Equation (3) can be expanded (up to ϕ^3) by substituting Equations (4)–(6) as follows:

$$\frac{\partial^2\phi}{\partial x^2} + n_+ = 1 + F_1\phi + F_2\phi^2 + F_3\phi^3 + \dots, \quad (7)$$

where

$$F_1 = \frac{\mu_2\varrho(2\kappa - 3) + (2\kappa - 1)(\mu_1 + \Lambda\rho)}{(2\kappa - 3)}, \quad F_2 = \frac{\mu_2\varrho^2(2\kappa - 3)^2 + (4\kappa^2 - 1)(\mu_1 - \Lambda\rho^2)}{2(2\kappa - 3)^2},$$

$$F_3 = \frac{\mu_2\varrho^3(2\kappa - 3)^3 + (4\kappa^2 - 1)(2\kappa + 3)(\mu_1 + \Lambda\rho^3)}{6(2\kappa - 3)^3},$$

where $\Lambda = \mu_1 + \mu_2 - 1$. Equations (1), (2), and (7) represent the IAW dynamics for this considered plasma model.

3. Derivation of the NLSE

We can employ the RPM to derive the NLSE and hence to study the MI of IAWs. The stretched (slow) co-ordinates can be written as

$$\xi = \epsilon(x - v_g t), \quad (8)$$

$$\tau = \epsilon^2 t, \quad (9)$$

where v_g and ϵ are denoted as the group speed and smallness parameter, respectively. So, the dependent variables can be expanded as

$$\begin{pmatrix} n_+ \\ u_+ \\ \phi \end{pmatrix} = \begin{pmatrix} 1 \\ 0 \\ 0 \end{pmatrix} + \sum_{m=1}^{\infty} \epsilon^m \sum_{L=-\infty}^{\infty} \begin{pmatrix} n_{+L}^{(m)} \\ u_{+L}^{(m)} \\ \phi_L^{(m)} \end{pmatrix} (\xi, \tau) \exp[iL(kx - \omega t)], \quad (10)$$

where $\omega(k)$ is the angular frequency (carrier wave number). The derivative operators are employed as

$$\frac{\partial}{\partial t} \rightarrow \frac{\partial}{\partial t} - \epsilon v_g \frac{\partial}{\partial \xi} + \epsilon^2 \frac{\partial}{\partial \tau}, \quad (11)$$

$$\frac{\partial}{\partial x} \rightarrow \frac{\partial}{\partial x} + \epsilon \frac{\partial}{\partial \xi}. \quad (12)$$

Thus, the first-order ($m = L = 1$) equation is obtained by using Equations (1), (2) and (7)–(12) and by selecting the co-efficients of ϵ ; the dispersion relation for IAWs is obtained as follows:

$$\omega^2 = k^2(1 + \eta k^2 + \eta F_1) / (k^2 + F_1). \quad (13)$$

Now, the reduced equation for the second order ($m = 2$ and $L = 1$) can be obtained as

$$n_{+1}^{(2)} = \frac{k^2}{\beta} \phi_1^{(2)} + \frac{2ik\omega(v_g k - \omega)}{\beta^2} \frac{\partial \phi_1^{(1)}}{\partial \xi}, \quad (14)$$

$$u_{+1}^{(2)} = \frac{\omega k}{\beta} \phi_1^{(2)} + \frac{i(v_g k - \omega)(\omega^2 + \eta k^2)}{\beta^2} \frac{\partial \phi_1^{(1)}}{\partial \xi}, \quad (15)$$

where $\beta = \omega^2 - \eta k^2$, and with the compatibility condition we obtain

$$v_g = (\omega^2 - \beta^2) / \omega k. \quad (16)$$

when $m = L = 2$, second-order harmonic amplitudes are found for the coefficient of ϵ in terms of $|\phi_1^{(1)}|^2$ as

$$n_{+2}^{(2)} = F_4 |\phi_1^{(1)}|^2, \quad (17)$$

$$u_{+2}^{(2)} = F_5 |\phi_1^{(1)}|^2, \quad (18)$$

$$\phi_2^{(2)} = F_6 |\phi_1^{(1)}|^2, \quad (19)$$

where

$$F_4 = k^2(\eta k^4 + 3\omega^2 k^2 + 2F_6 \beta^2) / 2\beta^3, \quad F_5 = \omega(F_4 \beta^2 - k^4) / \beta^2 k,$$

$$F_6 = [k^4(3\omega^2 + \eta k^2) - 2F_2 \beta^3] / 2\beta^2(4\beta k^2 + F_1 \beta - k^2).$$

Now, the expression of $n_{+0}^{(2)}$, $u_{+0}^{(2)}$ and $\phi_0^{(2)}$ in terms of $\phi_1^{(1)}$ is obtained for $m = 3$ with $L = 0$ and $m = 2$ with $L = 0$ as follows:

$$n_{+0}^{(2)} = F_7 |\phi_1^{(1)}|^2, \quad (20)$$

$$u_{+0}^{(2)} = F_8 |\phi_1^{(1)}|^2, \quad (21)$$

$$\phi_0^{(2)} = F_9 |\phi_1^{(1)}|^2, \quad (22)$$

where

$$F_7 = [k^2(2\omega v_g k + \omega^2 + \eta k^2) + F_9 \beta^2] / \beta^2 \beta_1, \quad F_8 = (F_7 v_g \beta^2 - 2\omega k^3) / \beta^2,$$

$$F_9 = [k^2(\omega^2 + \eta k^2 + 2\omega v_g k) - 2F_2 \beta^2 \beta_1] / \beta^2 (F_1 \beta_1 - 1),$$

where $\beta_1 = v_g^2 - \eta$. The standard NLSE is obtained by considering $m = 3$ and $l = 1$,

$$i \frac{\partial \Phi}{\partial \tau} + P \frac{\partial^2 \Phi}{\partial \xi^2} + Q |\Phi|^2 \Phi = 0, \quad (23)$$

where $\Phi = \phi_1^{(1)}$ is for simplicity. In Equation (23), P is the dispersion coefficient, which can be written as

$$P = \beta(4\eta k \omega - 3v_g \omega^2 - v_g k^2 \eta) / 2\omega^2 k, \quad (24)$$

and Q is the nonlinear coefficient, which can be written as

$$Q = \left[\beta^2 \{3F_3 + 2F_2(F_6 + F_9)\} - k^2 \{(\omega^2 + \eta k^2)(F_4 + F_7) - 2\omega k(F_5 + F_8)\} \right] / 2\omega k^2. \quad (25)$$

4. Modulational Instability and Envelope Solitons

The evolution of a fundamental wave whose amplitude follows Equation (23) depends on both P and Q , which are also dependent on η , ρ , q , μ_1 , and μ_2 . The stable and unstable parametric regimes of IAWs are determined by the sign of P and Q of Equation (23) [15,24–27]. When P and Q have the same sign (i.e., $P/Q > 0$), the evolution of the IAW amplitude is modulationally unstable in the presence of external perturbations. On the other hand, when P and Q have the opposite signs (i.e., $P/Q < 0$), the IAWs are modulationally stable in the presence of external perturbations. The plot of P/Q against k yields stable and unstable parametric regimes of the IAWs. The point at which the transition of P/Q curve intersects with the k -axis is known as the threshold or critical wave number k ($= k_c$) [24,25].

The bright (when $PQ > 0$) and dark (when $PQ < 0$) envelope solitonic solutions, respectively, can be written as [24,25]

$$\Phi(\xi, \tau) = \psi_0^{1/2} \operatorname{sech}[(\xi - U\tau)/J_1] \times \exp\left[i\left(U\xi + \Omega_0\tau - U^2\tau/2\right)/2P\right], \quad (26)$$

$$\Phi(\xi, \tau) = \psi_0^{1/2} \tanh[(\xi - U\tau)/J_2] \times \exp\left[i\left(U\xi + 2PQ\tau\psi_0 - U^2\tau/2\right)/2P\right], \quad (27)$$

where $J_1 = (2P\psi_0/Q)^{1/2}$, $J_2 = (2|P/Q|/\psi_0)^{1/2}$, ψ_0 is the amplitude of the localized pulse for both bright and dark envelope soliton, U is the propagation speed of the localized pulse, and Ω_0 is the oscillating frequency at $U = 0$. The pulse width for the bright and dark soliton is J_1 and J_2 , respectively. We observed the bright (for $k = 1.6$) and dark (for $k = 1.2$) envelope solitons, shown in Figure 1.

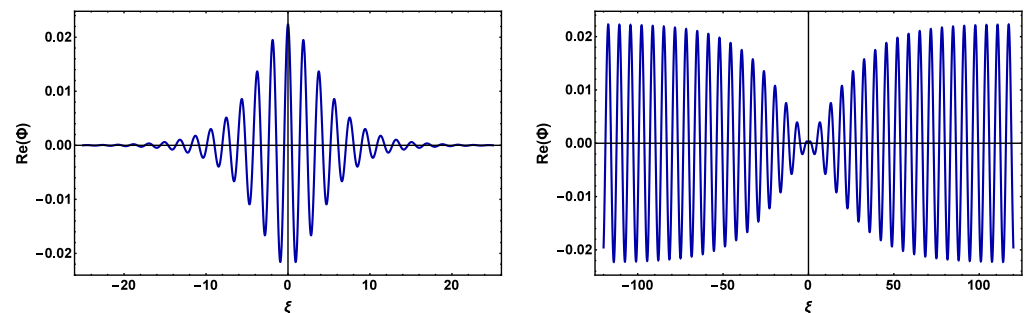


Figure 1. The bright (left panel) and dark (right panel) envelope solitons for $k = 1.6$ and $k = 1.2$, respectively, along with $\eta = 0.07$, $\rho = 1.2$, $q = 1.5$, $\kappa = 2$, $\mu_1 = 0.8$, $\mu_2 = 0.3$, $\tau = 0$, $\psi_0 = 0.0005$, $U = 0.2$, and $\Omega_0 = 0.4$.

5. Numerical Analysis

The presence of two-temperature electrons with number density as well as temperature can be observed in Saturn's magnetosphere [5,6,8,10,11,28], Earth's magnetosphere [29], Auroral plasma [2,30], rf-heated plasma [31], tandem mirror experiments [32], and sputtering magnetron plasma [33], etc. Saturn's magnetosphere has three regions: the inner magnetosphere ($R \leq 9R_s$), intermediate magnetosphere ($9R_s < R < 13R_s$), and outer magnetosphere ($\geq 13R_s$), where $R_s \approx 60,300$ km is the radius of Saturn. Schippers et al. [28] analyzed the MIMI/LEMMS and CAPS/ELS data from the Cassini spacecraft orbiting Saturn over a range of $5.4\text{--}20R_s$, which can be found in Table 1.

Table 1. Parameter values derived from Schippers et al. corresponding to Saturn’s magnetosphere.

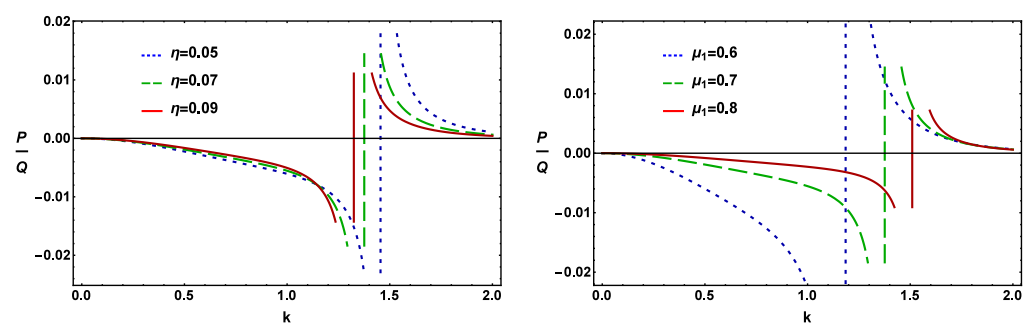
| $R (R_s)$ | $T_{e2} (eV)$ | $T_{e1} (eV)$ | $n_{e2} (cm^{-3})$ | $n_{e1} (cm^{-3})$ |
|-----------|---------------|---------------|--------------------|--------------------|
| 5.40 | 1.8 | 300 | 10.5 | 0.02 |
| 6.30 | 2.0 | 400 | 10.5 | 0.01 |
| 9.80 | 8.0 | 1100 | 2.5 | 0.07 |
| 12.0 | 6.0 | 1200 | 1.0 | 0.11 |
| 13.1 | 10.2 | 1000 | 0.21 | 0.18 |
| 14.0 | 30 | 900 | 0.15 | 0.10 |
| 15.2 | 70 | 900 | 0.25 | 0.10 |
| 17.8 | 28 | 1000 | 0.15 | 0.07 |

Several authors numerically analyzed the effects of two-temperature (hot and cold) electrons following iso-thermal [4,34] or non-thermal [3,5,6,8–11] distribution on the dynamics of space [3–6,8–11] and laboratory [31,33,34] plasma systems under these assumptions: $T_{e1} > T_{e2}$ and $n_{e10} > n_{e20}$ [4,8,10,11,31,34] or $n_{e10} = n_{e20}$ [5,10,11] or $n_{e10} < n_{e20}$ [6,8,33,34]. In our present investigation, we considered for our numerical analysis that $T_{e1} = T_p = (10\sim 1000)T_{e2}$, $T_+ = 0.1T_{e2}$ [10,31], $Z = 1\text{--}20$ [3,5,8,9], $n_{e10} > n_{e20}$, $n_{e10} = n_{e20}$, $n_{e10} < n_{e20}$, and small fraction of positrons.

We graphically examined the effects of the temperature of the warm ion and super-thermal electron as well as the charge state of the warm ion in recognizing the stable and unstable domains of the IAWs in the left panel of Figure 2, and it is clear from this figure that: (a) the stable domain decreases with the increase in the value of warm ion temperature but increases with the increase in the value of super-thermal electron temperature when the charge state of the warm ion remains constant; (b) the stable domain increases with Z_+ for the constant value of T_+ and T_{e1} (via $\eta = 3T_+/Z_+T_{e1}$). So, the charge state and temperature of the warm ion play an opposite role in manifesting the stable and unstable domains of the IAWs.

Both stable (i.e., $k < k_c$) and unstable (i.e., $k > k_c$) domains for the IAWs can be observed from the right panel of Figure 2, and it is obvious from this figure that: (a) when $\mu_1 = 0.6, 0.7$, and 0.8 , then the corresponding value of k_c is 1.20 (dotted blue curve), 1.40 (dashed green curve), and 1.50 (solid red curve); (b) k_c is shifted to higher values with the increase (decrease) in n_{e10} (n_{+0}) when the value of Z_+ is constant. Finally, μ_1 would cause the stable domain of IAWs to increase.

We graphically analyzed the effect of temperature of the super-thermal electron and positron (via ρ) on the stability conditions of IAWs in the left panel of Figure 3. It can be observed from this figure that the stable domain increases with an increase (decrease) in the value of super-thermal electron (positron) temperature. The right panel of Figure 3 illustrates the effects of the super-thermality of plasma species in the stable and unstable parametric domains. It is clear from Figure 3 that for large values of κ , the IAWs become unstable for small values of k while for small values of κ , the IAWs become unstable for large values of k .

**Figure 2.** Plot of P/Q vs. k for the change of η (left panel) and μ_1 (right panel) when $\rho = 1.2$, $q = 1.5$, $\kappa = 2$, and $\mu_2 = 0.5$.

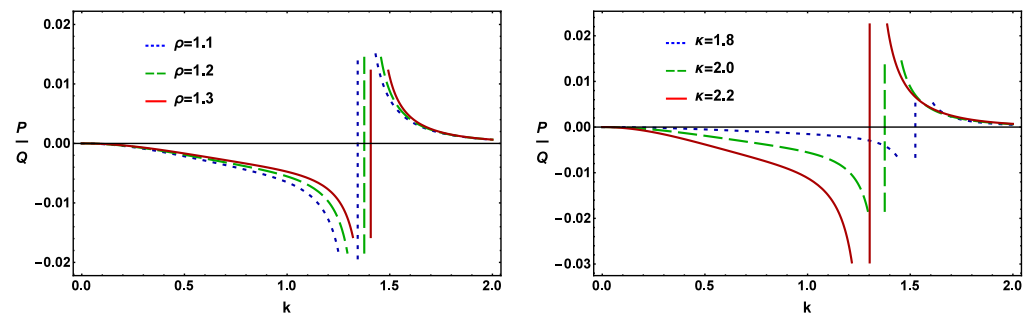


Figure 3. Plot of P/Q vs. k for the change of ρ (left panel) and κ (right panel) when $\eta = 0.07$, $q = 1.5$, $\mu_1 = 0.7$, and $\mu_2 = 0.5$.

6. Conclusions

We studied the stability of IAWs in an unmagnetized realistic space plasma system containing warm ions, iso-thermal electrons, κ -distributed electrons and positrons. The RPM was used to derive the NLSE. The existence of both stable and unstable regions of IAWs was found, and the interaction between the k_c with various plasma parameters (i.e., η , μ_1 , ρ , and κ , etc.) was also observed. The fluid approximations (which reduce the kinetic theory to a fluid theory) used in our present investigation are valid as long as one can neglect the effects of individual plasma particle dynamics [12,35]. The fluid theory, which is a common and popular approach for investigating many linear and nonlinear phenomena like our present investigation, is suitable in understanding the latter, in interpreting most of the experimental observations and in designing new laboratory experiments [12]. However, the kinetic theory is essential for some plasma phenomena such as Bernstein waves, the formation of local instabilities due to the fluctuating local electric field and the anisotropic effects associated with ion-acoustic waves, Landau damping etc. [12,35]. One can, of course, carry out our present work by employing the kinetic theory, but obtain the same results with the same basic physics under some valid approximations. Finally, these results will be applicable in understanding the conditions of the MI of IAWs and associated envelope solitons in both space [3–6,8–11] and laboratory environments [4,12].

Author Contributions: All authors contributed equally to complete this work. All authors have read and agreed to the published version of the manuscript.

Funding: The research received no external funding.

Institutional Review Board Statement: Not applicable.

Informed Consent Statement: Not applicable.

Data Availability Statement: Data sharing not applicable—no new data generated.

Conflicts of Interest: The authors declare no conflict of interest.

References

1. Ergun, R.E.; Carlson, C.W.; McFadden, J.P.; Mozer, F.S.; Delory, G.T.; Peria, W.; Chaston, C.C.; Temerin, M.; Elphic, R.; Strangeway, R.; et al. FAST satellite wave observations in the AKR source region. *Geophys. Res. Lett.* **1998**, *25*, 2061. [\[CrossRef\]](#)
2. Temerin, M.; Cerny, K.; Lotko, W.; Mozer, F.S. Observations of double layers and solitary waves in the auroral plasma. *Phys. Rev. Lett.* **1982**, *48*, 1175. [\[CrossRef\]](#)
3. Shahmansouri, M.; Alinejad, H. Electrostatic wave structures in a magnetized superthermal plasma with two-temperature electrons. *Phys. Plasmas* **2013**, *20*, 082130. [\[CrossRef\]](#)
4. Rehman, M.A.; Mishra, M.K. Ion-acoustic Gardner solitons in electron-positron-ion plasma with two-electron temperature distributions. *Phys. Plasmas* **2016**, *23*, 012302. [\[CrossRef\]](#)
5. Kourakis, I.; Shukla, P.K. Ion-acoustic waves in a two-electron-temperature plasma: Oblique modulation and envelope excitations. *J. Phys. A Math. Gen.* **2003**, *36*, 11901. [\[CrossRef\]](#)
6. Alinejad, H.; Mahdavi, M.; Shahmansouri, M. Modulational instability of ion-acoustic waves in a plasma with two-temperature kappa-distributed electrons. *Astrophys. Space Sci.* **2014**, *352*, 0571. [\[CrossRef\]](#)

7. Ali, R.; Saha, A.; Chatterjee, P. Dynamics of the positron acoustic waves in electron-positron-ion magnetoplasmas. *Indian J. Phys.* **2017**, *91*, 689. [[CrossRef](#)]
8. Panwar, A.; Ryu, C.M.; Bains, A.S. Oblique ion-acoustic cnoidal waves in two temperature superthermal electrons magnetized plasma. *Phys. Plasmas* **2014**, *21*, 0122105. [[CrossRef](#)]
9. Shalini; Saini, N.S.; Misra, A.P. Modulation of ion-acoustic waves in a nonextensive plasma with two-temperature electrons. *Phys. Plasmas* **2015**, *22*, 092124. [[CrossRef](#)]
10. Baluku, T.K.; Hellberg, M.A. Ion acoustic solitons in a plasma with two-temperature kappa-distributed electrons. *Phys. Plasmas* **2012**, *19*, 012106. [[CrossRef](#)]
11. Baluku, T.K.; Hellberg, M.A.; Mace, R.L. Electron acoustic waves in double-kappa plasmas: Application to Saturn's magnetosphere. *J. Geophys. Res.* **2011**, *116*, A04227. [[CrossRef](#)]
12. Chen, F.F. *Introduction to Plasma Physics and Controlled Fusion*, 3rd ed.; Springer: Cham, Switzerland, 2016.
13. Chowdhury, N.A.; Mannan, A.; Hasan, M.M.; Mamun, A.A. Heavy ion-acoustic rogue waves in electron-positron multi-ion plasmas. *Chaos* **2017**, *27*, 093105. [[CrossRef](#)]
14. Chowdhury, N.A.; Hasan, M.M.; Mannan, A.; Mamun, A.A. Nucleus-acoustic envelope solitons and their modulational instability in a degenerate quantum plasma system. *Vacuum* **2018**, *147*, 31. [[CrossRef](#)]
15. Jahan, S.; Haque, M.N.; Chowdhury, N.A.; Mannan, A.; Mamun, A.A. Ion-acoustic rogue waves in double pair plasma having non-extensive particles. *Universe* **2021**, *7*, 63. [[CrossRef](#)]
16. Paul, S.N.; Chowdhury, A.R.; Paul, I. Modulation instability of bright envelope soliton and rogue waves in ultra-relativistic degenerate dense electron-ion-positron plasma. *Plasma Phys. Rep.* **2019**, *45*, 1011. [[CrossRef](#)]
17. Sittler, E.C.; Ogilvie, K.W.; Scudder, J.D. Survey of low-energy plasma electrons in Saturn's magnetosphere: Voyagers 1 and 2. *J. Geophys. Res.* **1983**, *88*, 8847. [[CrossRef](#)]
18. Young, D.T.; Berthelier, J.-J.; Blanc, M.; Burch, J.L.; Bolton, S.; Coates, A.J.; Crary, F.J.; Goldstein, R.; Grande, M.; Hill, T.W.; et al. Composition and dynamics of plasma in Saturn's magnetosphere. *Science* **2005**, *307*, 1262. [[CrossRef](#)]
19. Pottellette, R.; Ergun, R.E.; Treumann, R.A.; Treumann, R.A.; Berthomier, T.M.; Carlson, C.W.; McFadden, J.P.; Roth, I. Modulated electron-acoustic waves in auroral density cavities: FAST observations. *Geophys. Res. Lett.* **1999**, *26*, 2629. [[CrossRef](#)]
20. Vasyliunas, V.M. A survey of low-energy electrons in the evening sector of the magnetosphere with OGO 1 and OGO 3. *J. Geophys. Res.* **1968**, *73*, 2839. [[CrossRef](#)]
21. Ahmed, N.; Mannan, A.; Chowdhury, N.A.; Mamun, A.A. Electrostatic rogue waves in double pair plasmas. *Chaos* **2018**, *28*, 123107. [[CrossRef](#)]
22. Noman, A.A.; Islam, M.K.; Hassan, M.; Banik, S.; Chowdhury, N.A.; Mannan, A.; Mamun, A.A. Dust-ion-acoustic rogue waves in a dusty plasma having super-thermal electrons. *Gases* **2021**, *1*, 106–116. [[CrossRef](#)]
23. Heera, N.M.; Akter, J.; Tamanna, N.K.; Chowdhury, N.A.; Rajib, T.I.; Sultana, S.; Mamun, A.A. Ion-acoustic shock waves in a magnetized plasma featuring super-thermal distribution. *AIP Adv.* **2021**, *11*, 055117. [[CrossRef](#)]
24. Kourakis, I.; Shukla, P.K. Exact theory for localized envelope modulated electrostatic wavepackets in space and dusty plasmas. *Nonlinear Proc. Geophys.* **2005**, *12*, 407. [[CrossRef](#)]
25. Sultana, S.; Kourakis, I. Electrostatic solitary waves in the presence of excess superthermal electrons: Modulational instability and envelope soliton modes. *Plasma Phys. Control. Fusion* **2011**, *53*, 045003. [[CrossRef](#)]
26. Rahman, M.H.; Chowdhury, N.A.; Mannan, A.; Mamun, A.A. Dust-acoustic rogue waves in an electron-positron-ion-dust plasma medium. *Galaxies* **2021**, *9*, 31. [[CrossRef](#)]
27. Sikta, J.N.; Chowdhury, N.A.; Mannan, A.; Mamun, A.A. Electrostatic dust-acoustic rogue waves in an electron depleted dusty plasma. *Plasma* **2021**, *4*, 230–238. [[CrossRef](#)]
28. Schippers, P.; Blanc, M.; Andre, N.; Dandouras, I.; Lewis, G.R.; Gilbert, L.K.; Persoon, A.M.; Krupp, N.; Gurnett, D.A.; Coates, A.J.; et al. Multi-instrument analysis of electron populations in Saturn's magnetosphere. *J. Geophys. Res.* **2008**, *113*, A07208. [[CrossRef](#)]
29. Gaffey, J.D.; LaQuey, R.E. Upper hybrid resonance in the magnetosphere. *J. Geophys. Res.* **1976**, *81*, 595. [[CrossRef](#)]
30. Bostrom, R.; Gustafsson, G.; Holback, B.; Holmgren, G.; Koskinen, H.; Kintner, P. Characteristics of solitary waves and weak double layers in the magnetospheric plasma. *Phys. Rev. Lett.* **1988**, *61*, 82. [[CrossRef](#)]
31. Nishida, Y.; Nagasawa, T. Excitation of ion-acoustic rarefactive solitons in a two-electron temperature plasma. *Phys. Fluids* **1986**, *29*, 345. [[CrossRef](#)]
32. Kenser, J. Axisymmetric, wall-stabilized tandem mirrors. *Nucl. Fusion* **1985**, *25*, 275.
33. Sheridan, T.E.; Goeckner, M.J.; Goree, J. Observation of two-temperature electrons in a sputtering magnetron plasma. *J. Vac. Sci. Tech. A* **1991**, *9*, 688. [[CrossRef](#)]
34. Baboolal, S.; Bharuthram, R.; Hellberg, M.A. Arbitrary-amplitude theory of ion-acoustic solitons in warm multi-fluid plasmas. *J. Plasma Phys.* **1989**, *41*, 341. [[CrossRef](#)]
35. Krall, N.A.; Trivelpiece, A.W. *Principles of Plasma Physics*; McGraw-Hill: New York, NY, USA, 1973.